ADVANCED MATERIALS

Supporting Information

for *Adv. Mater.*, DOI: 10.1002/adma.201602338

Selective Adsorption of Sulfur Dioxide in a Robust Metal–Organic Framework Material

Mathew Savage, Yongqiang Cheng, Timothy L. Easun, Jennifer E. Eyley, Stephen P. Argent, Mark R. Warren, William Lewis, Claire Murray, Chiu C. Tang, Mark D. Frogley, Gianfelice Cinque, Junliang Sun, Svemir Rudic´, Richard T. Murden, Michael J. Benham, Andrew N. Fitch, Alexander J. Blake, Anibal J. Ramirez-Cuesta, Sihai Yang, and Martin Schröder**

Supplementary Information

Selective Adsorption of Sulphur Dioxide in a Robust Metal-Organic Framework Material

Mathew Savage,[1] Yongqiang Cheng,[2] Timothy L. Easun,[3] Jennifer E. Eyley,[1] Stephen P. Argent,[4] Mark R. Warren,[5] William Lewis,[4] Claire Murray,[5] Chiu C. Tang,[5] Mark D. Frogley,[5] Gianfelice Cinque,[5] Junliang Sun,[6] Svemir Rudić,[7] Richard T. Murden,[8] Michael J. Benham,[8] Andrew N. Fitch,[9] Alexander J. Blake,[4] Anibal J. Ramirez-Cuesta,[2] Sihai Yang[1]* and Martin Schröder[1]*

[1] *School of Chemistry, University of Manchester, Manchester, M13 9PL (UK)*

E-mail: Sihai.Yang@manchester.ac.uk; M.Schroder@manchester.ac.uk

[2] *The Chemical and Engineering Materials Division (CEMD), Neutron Sciences Directorate, Oak Ridge National Laboratory, Oak Ridge, TN 37831 (USA)*

[3] *School of Chemistry, Cardiff University, Cardiff, CF10 3XQ (UK)*

[4] *School of Chemistry, University of Nottingham, University Park, Nottingham, NG7 2RD (UK)*

[5] *Diamond Light Source, Harwell Science Campus, Oxfordshire, OX11 0DE (UK)*

[6] *College of Chemistry and Molecular Engineering, Peking University, Beijing, 100871 (China)*

[7] *ISIS Neutron Facility, STFC Rutherford Appleton Laboratory, Chilton, Oxfordshire, OX11 0QX (UK)*

[8] *Hiden Isochema, 422 Europa Boulevard, Warrington, WA5 7TS (UK)*

[9] *European Synchrotron Radiation Facility, Grenoble, 38043 (France)*

Contents

Contents	2
Materials and Measurements	3
Synthesis of MFM-300(In)	3
Synthesis of Single Crystals of MFM-300(In)	3
Calculation of Surface Coverage of –OH Groups.	3
Stability of MFM-300(In) to SO_2	4
Gas Adsorption Measurements	9
Analysis and Derivation of the Isosteric Heats of Adsorption	12
Fitting of Isotherm Data to the Langmuir-Freundlich Model	13
Analysis and Derivation of the Ideal Adsorption Solution Theory (IAST) Selectivity	14
X-Ray Powder Diffraction (PXRD) of SO_2-Loaded MFM-300(In)	17
Crystal Structure Data	18
X-Ray Powder Diffraction (PXRD) of High Pressure CO_2-loaded MFM-300(In)	20
Single Crystal X-Ray Diffraction of CO_2-Loaded MFM-300(In) at Ambient Pressure	22
Desolvated MFM-300(In)	23
MFM-300(In).4CO_2	23
Neutron Scattering Measurements	27
Modelling of INS Spectra	28
Infrared (IR) Microscopy of CO_2- and SO_2-Loaded MFM-300(In) at Ambient Pressures	29
CO_2 binding	29
SO_2 binding	30
References	33

Materials and Measurements

All reagents and solvents were purchased from commercial suppliers and used without further purification. Elemental analyses (C, H and N) were carried out on a CE-440 elemental analyser. SEM samples were gold coated to avoid charging, and images were collected using an FEI XL30 ESEM.

Synthesis of MFM-300(In)

H_4L (330 mg, 1.00 mmol) and $In(NO_3)_3{\cdot}5H_2O$ (585 mg, 1.50 mmol) were mixed and dispersed in a DMF/MeCN mixture (30 mL, 2:1 v/v) in a 250 mL glass pressure reactor. The white slurry was acidified with conc. nitric acid (65 % 1.0 mL), the vessel sealed and heated at 80 °C for 48 hours. The resultant flaky white precipitate was then washed with DMF and dried briefly in air. Yield 347 mg. The acetone-exchanged material was prepared by suspending the as-synthesised sample in an excess of acetone for 5 days with frequent exchange of solvent.

Synthesis of Single Crystals of MFM-300(In)

Single crystals of $[In_2(OH)_2(C_{16}O_8H_6)]$.solvate MFM-300(In).solvate were synthesised by the method of Qian *et al*.[1]

Calculation of Surface Coverage of –OH groups

The concentration of surface –OH groups in MFM-300(In) has been calculated.

$[In(OH)(C_{16}H_6O_8)_{0.5}]$ Mt = 293.93; BET = 1071 $m^2\ g^{-1}$ = 1071 x 10^{18} (100 $Å^2\ g^{-1}$)

$1/293.93 * 6.02 * 10^{23} /(1071 * 10^{18})$ = 1.91 OH/100 $Å^2$

Stability of MFM-300(In) to SO_2

The stability of MFM-300(In) to SO_2 in a range of dry and humid conditions was investigated by exposing the material to SO_2 gas, and as suspensions to 0.1 and 0.5 M solutions of H_2SO_3 (as aqueous SO_2), and H_2SO_4. Powder X-ray diffraction and SEM micrographs confirm the absence of marked degradation of sample quality following exposure to these corrosive environments.

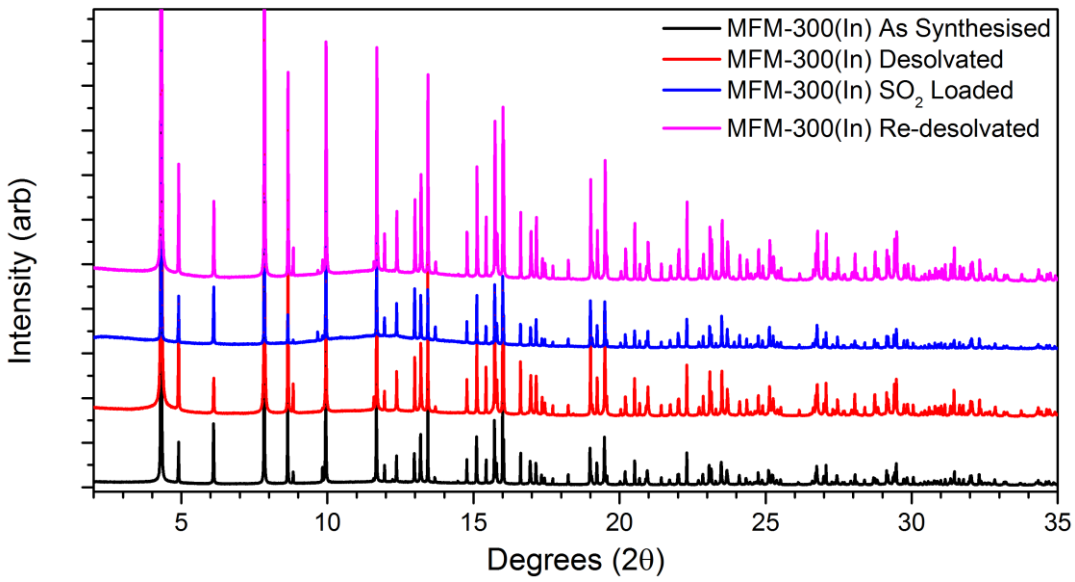

Figure S1. Powder X-ray diffraction patterns of MFM-300(In) as-synthesised, upon desolvation, dosing to 1 bar of SO_2 and re-desolvation. Measurement carried out at I11 at the Diamond Light Source using 0.826126(2) Å radiation.

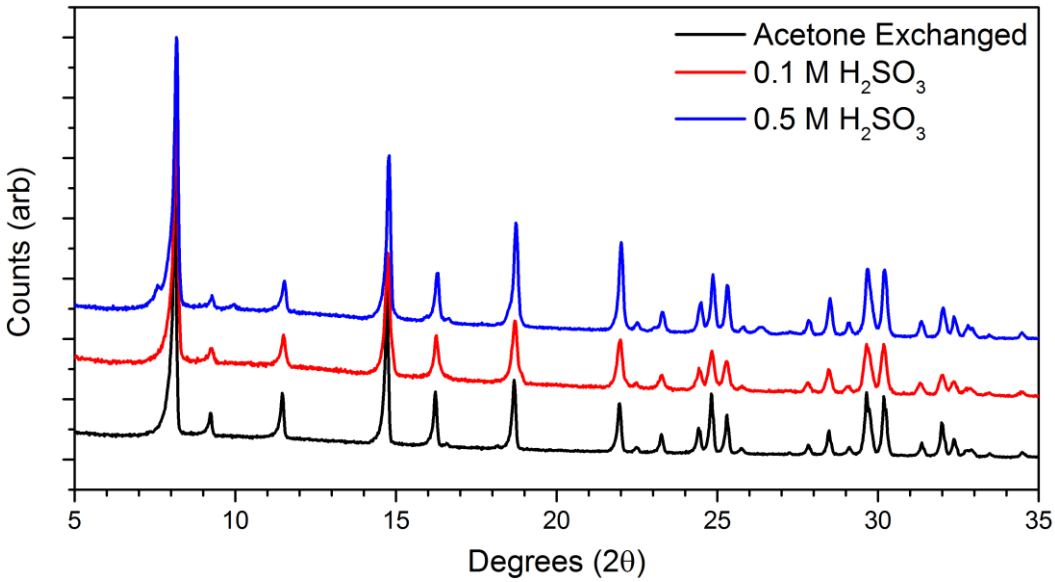

Figure S2. Powder X-ray diffraction patterns of MFM-300(In) upon exposure to 0.1 and 0.5 M H_2SO_3 for 1 hour.

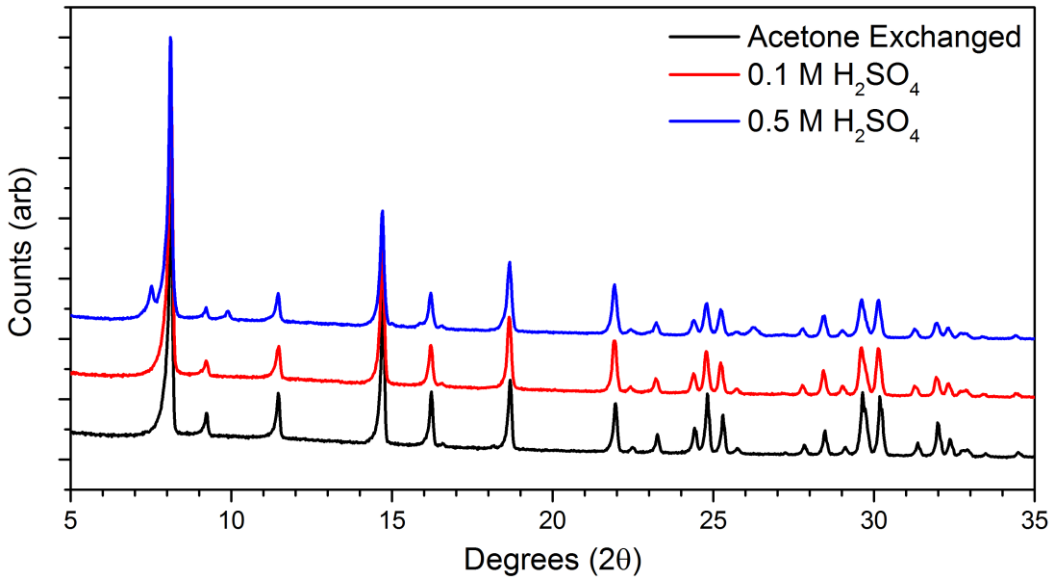

Figure S3. Powder X-ray diffraction patterns of MFM-300(In) upon exposure to 0.1 and 0.5 M H_2SO_4 for 1 hour.

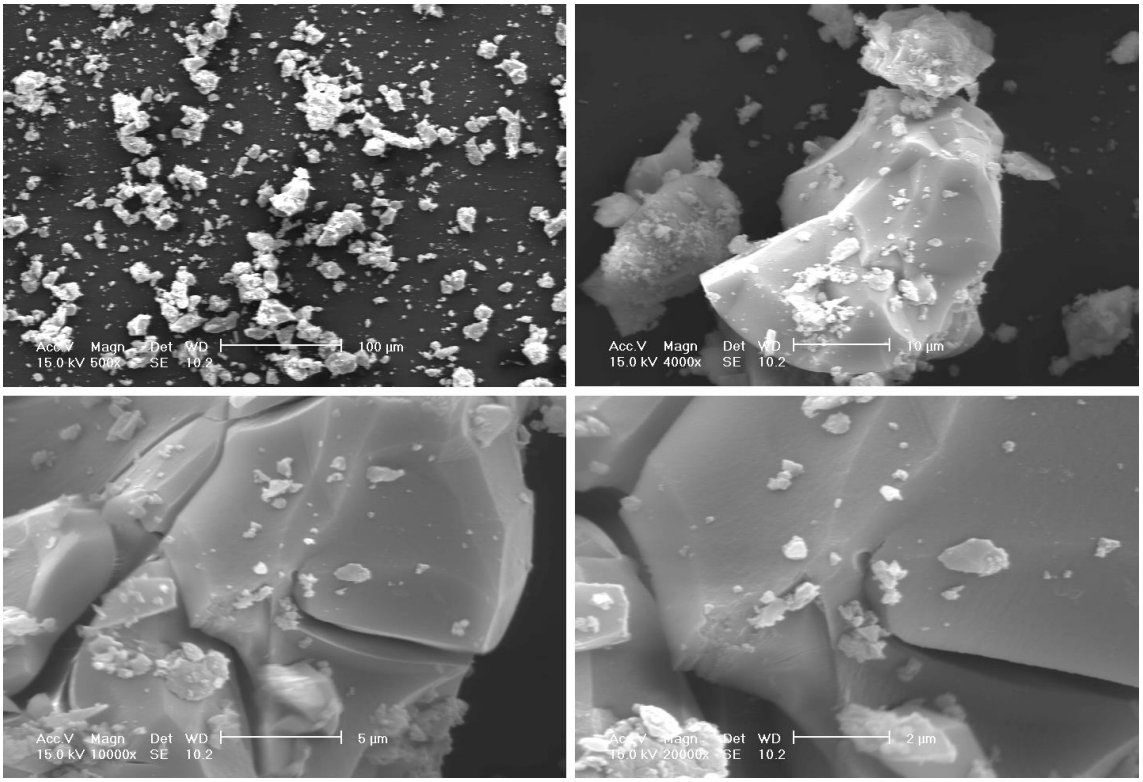

Figure S4. SEM micrographs of MFM-300(In) at a) 500, b) 4000, c) 10000 and d) 20000 x magnification.

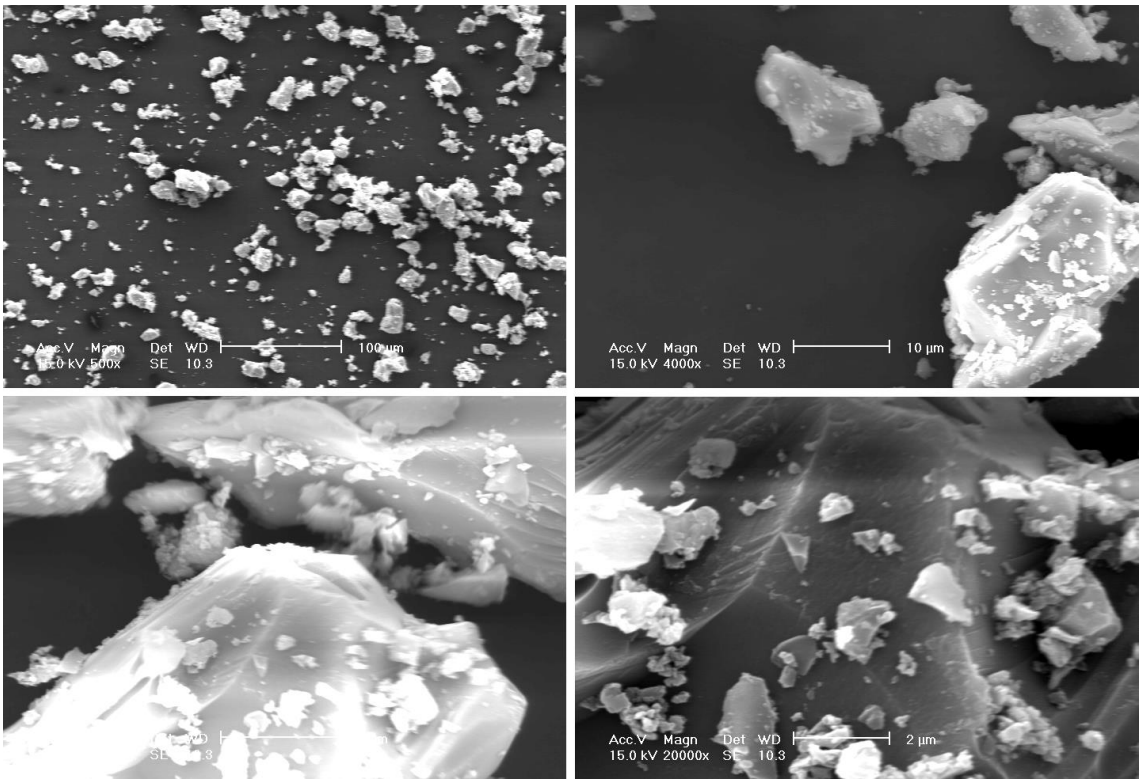

Figure S5. SEM micrographs of MFM-300(In) treated with SO_2 at a) 500, b) 4000, c) 10000 and d) 20000 x magnification.

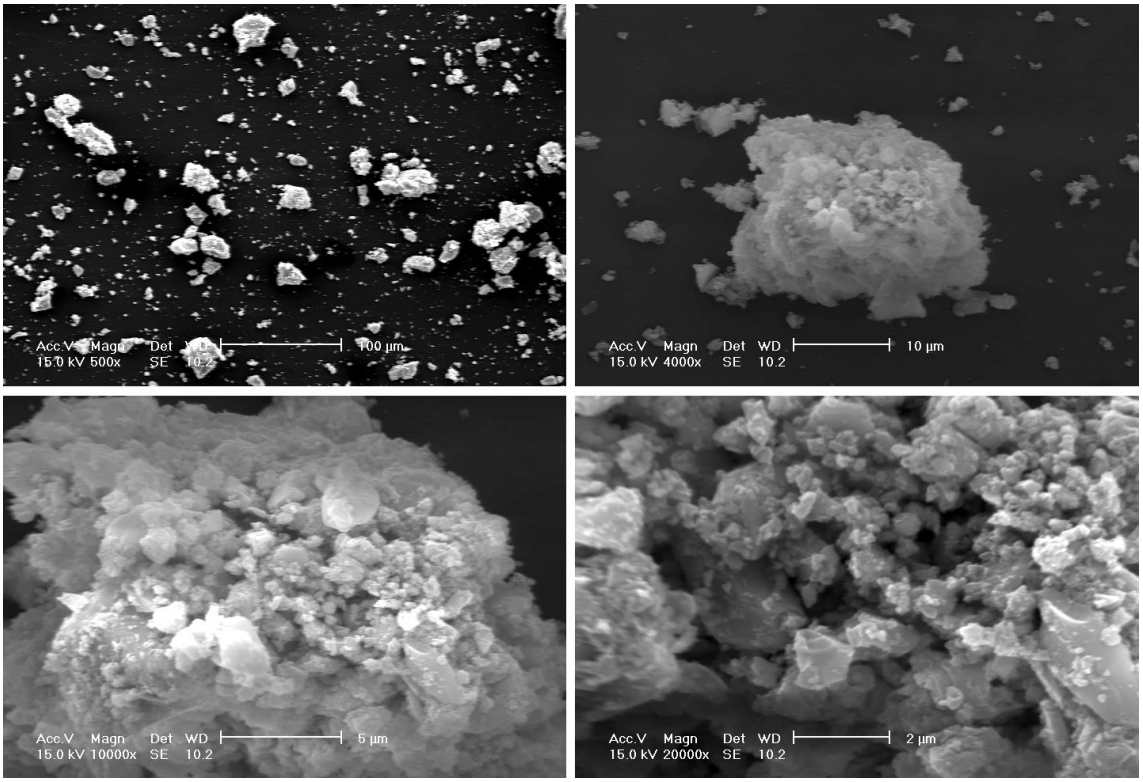

Figure S6. SEM micrographs of MFM-300(In) treated with 0.1 M H_2SO_3 for 1 hour at a) 500, b) 4000, c) 10000 and d) 20000 x magnification.

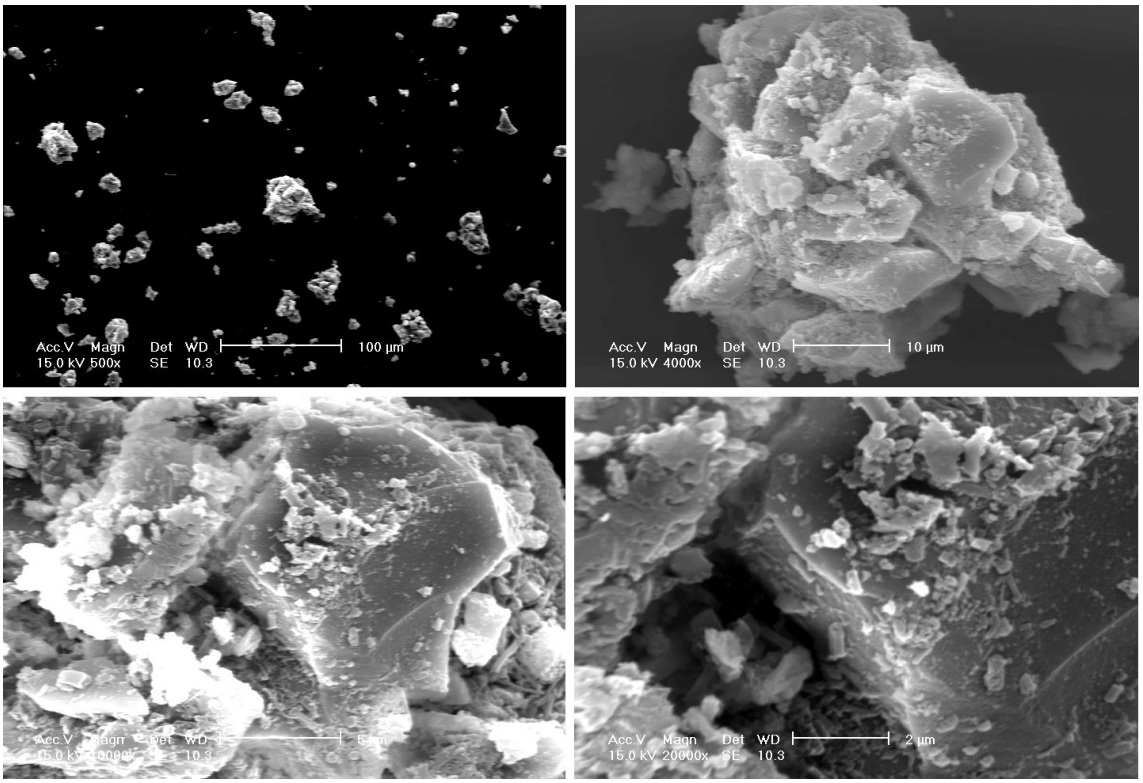

Figure S7. SEM micrographs of MFM-300(In) treated with 0.5 M H_2SO_3 for 1 hour at a) 500, b) 4000, c) 10000 and d) 20000 x magnification.

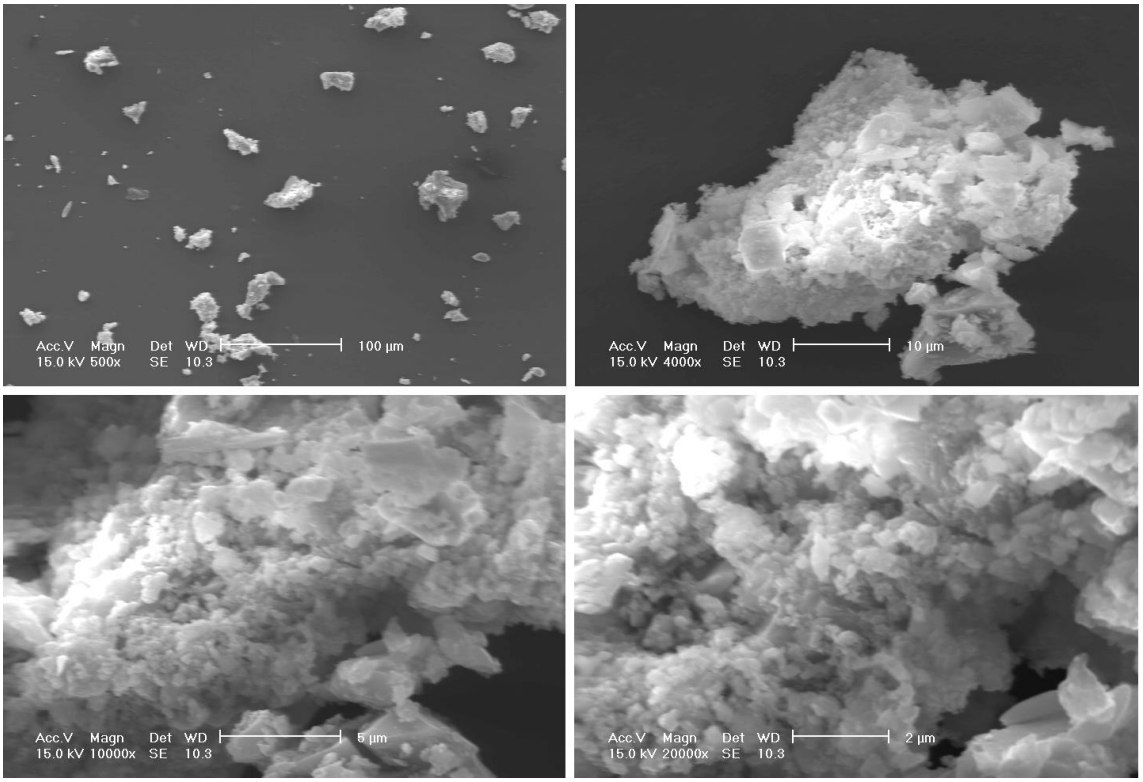

Figure S8. SEM micrographs of MFM-300(In) treated with 0.1 M H_2SO_4 for 1 hour at a) 500, b) 4000, c) 10000 and d) 20000 x magnification.

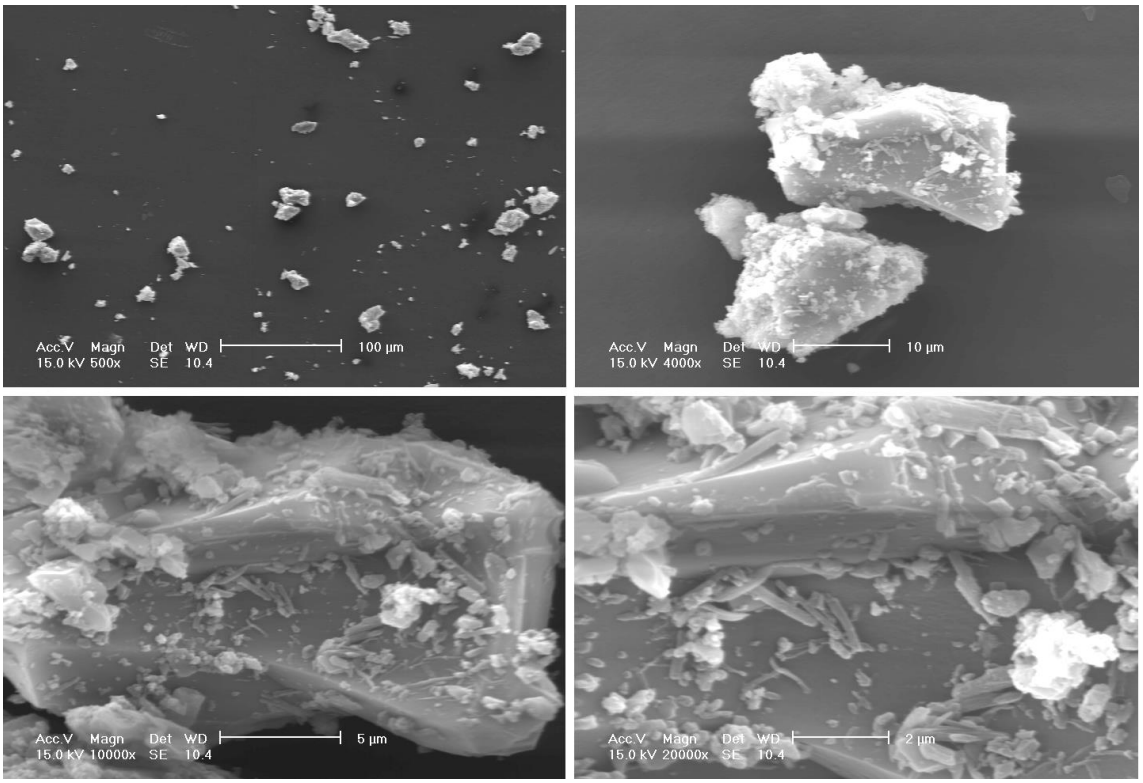

Figure S9. SEM micrographs of MFM-300(In) treated with 0.5 M H_2SO_4 for 1 hour at a) 500, b) 4000, c) 10000 and d) 20000 x magnification.

Gas Adsorption Measurements

N_2, CH_4, and CO_2 isotherms (0 – 4 and 0 – 20 bar, respectively) were recorded at 273 – 303 K on an IGA-003 system (Hiden Isochema, Warrington, UK. SO_2 (0-1 bar) and high pressure N_2 (0 – 180 bar) isotherms were recorded at 273 – 348 K on a XEMIS system (Hiden Isochema, Warrington, UK). In all cases the desolvated sample was generated *in situ* within the reactor of the instrument by heating the acetone-exchanged sample to 120 ºC under vacuum (1×10^{-6} mbar) until the sample mass had stabilised. Research grade N_2 and CO_2 and SO_2 were purchased from BOC and used as received.

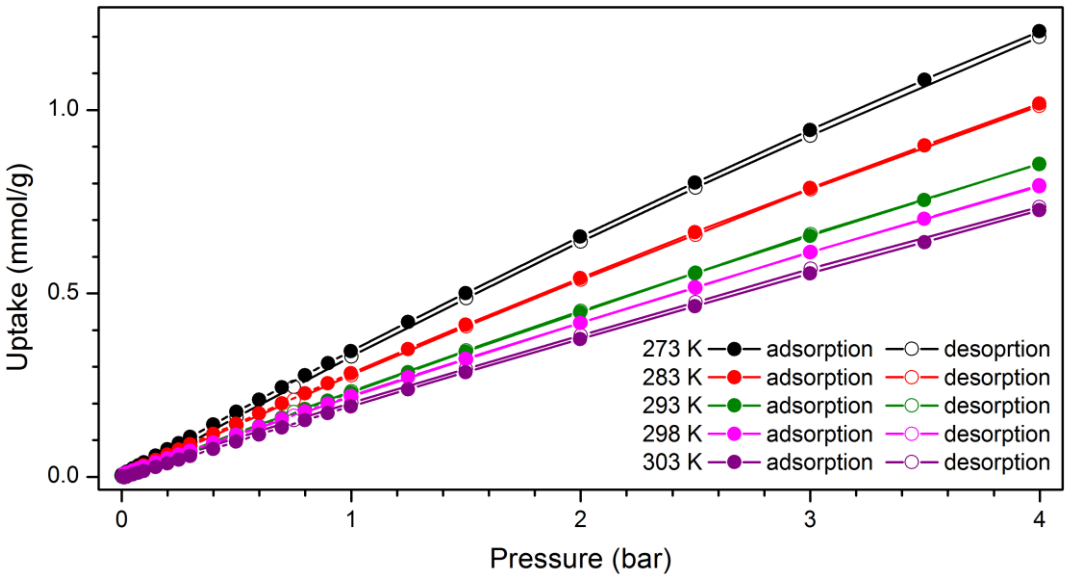

Figure S10. Low pressure N_2 adsorption isotherms for MFM-300(In).

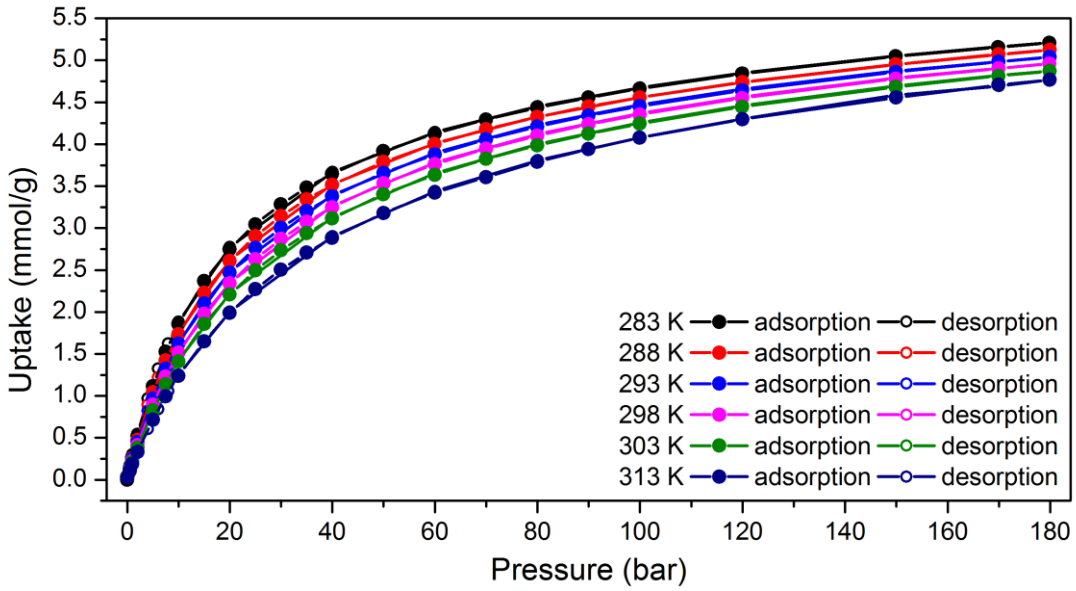

Figure S11. High pressure N_2 adsorption isotherms for MFM-300(In).

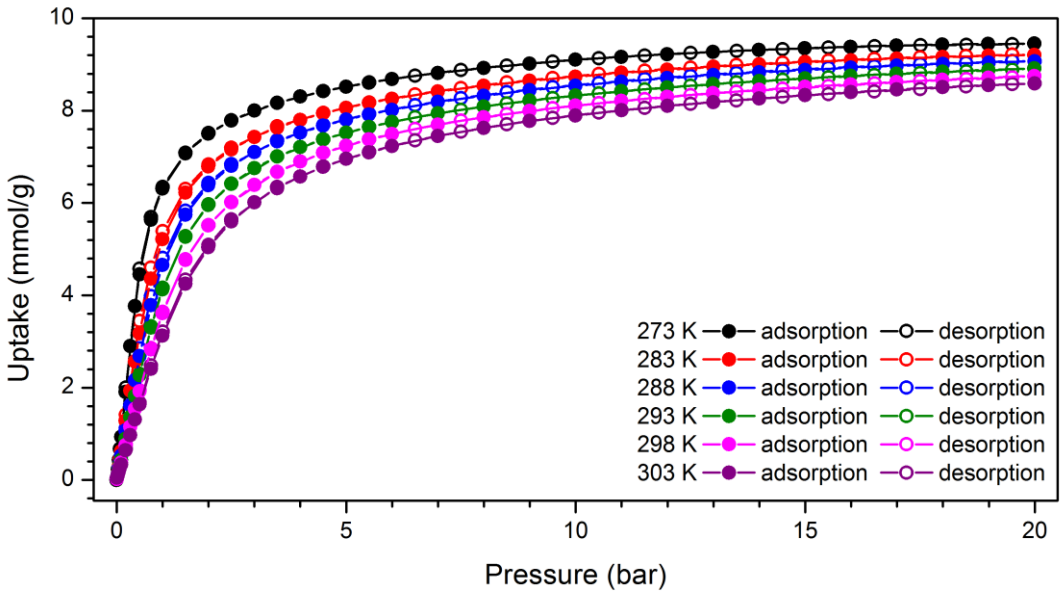

Figure S12. CO_2 adsorption isotherms for MFM-300(In).

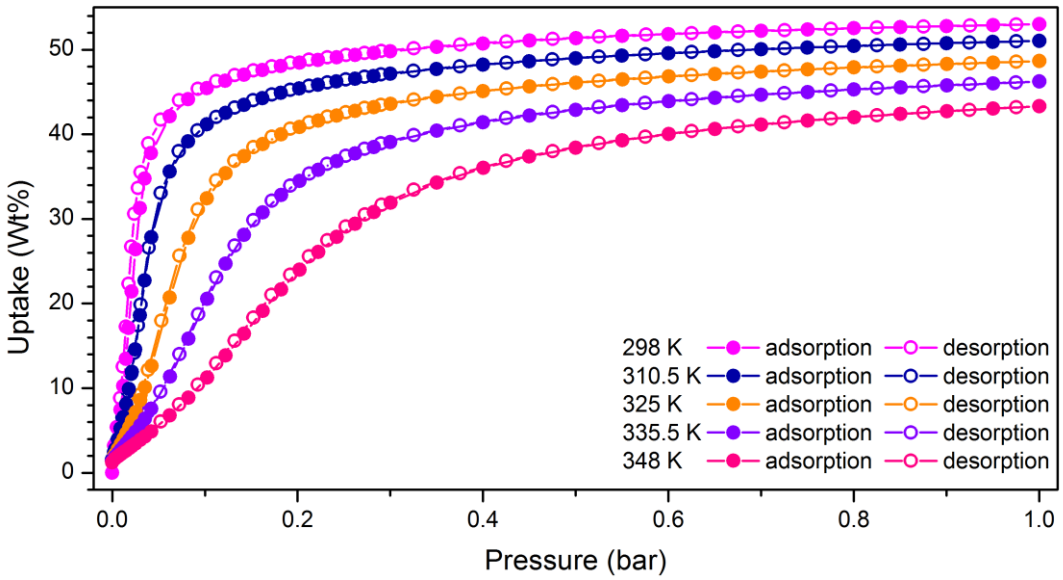

Figure S13. SO_2 adsorption isotherms for MFM-300(In).

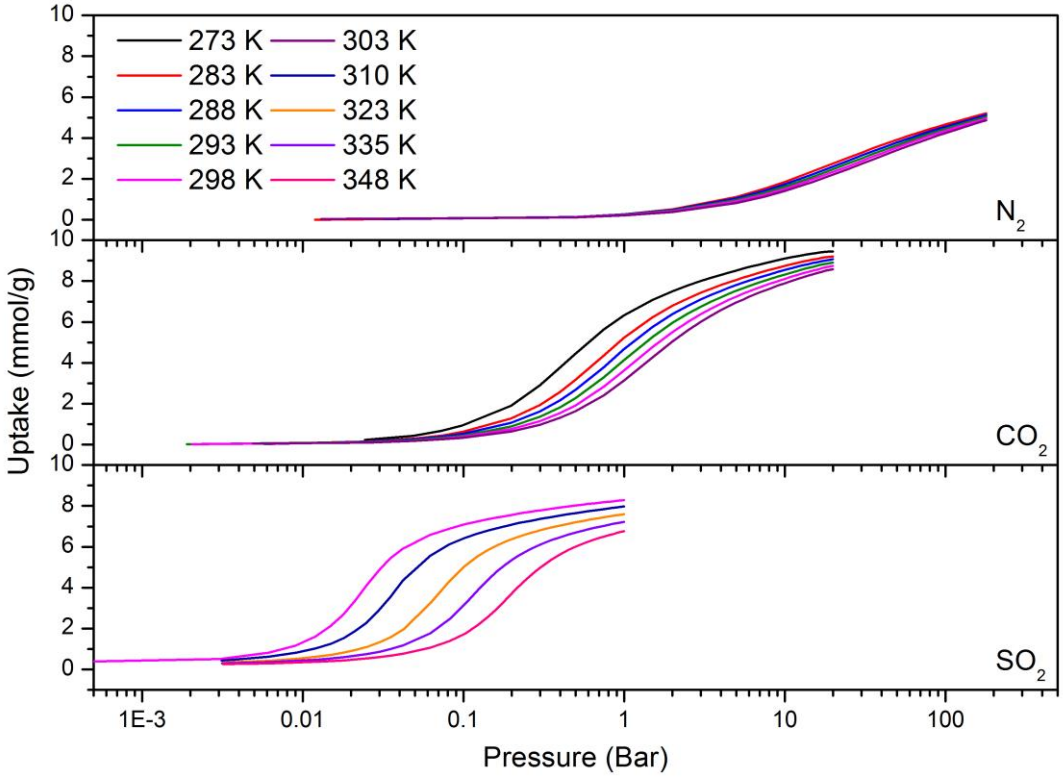

Figure S14. Comparison of the N_2, CO_2 and SO_2 adsorption isotherms at 273-348 K plotted using a logarithmic scale confirming the absence of distinct adsorption steps.

Analysis and Derivation of the Isosteric Heats of Adsorption

To estimate the isosteric enthalpies (ΔH) for N_2, CO_2 and SO_2 adsorption, isotherms at 273-308 K were fitted to the Van t' Hoff equation;

$$lnP = \frac{-\Delta H}{RT} + \frac{\Delta S}{R} \quad \textbf{(1)}$$

where P is pressure in Pa, T is the temperature, and R is the ideal gas constant. All linear fittings show R^2 above 0.99 confirming the consistency of the isotherm data and of the fitting.

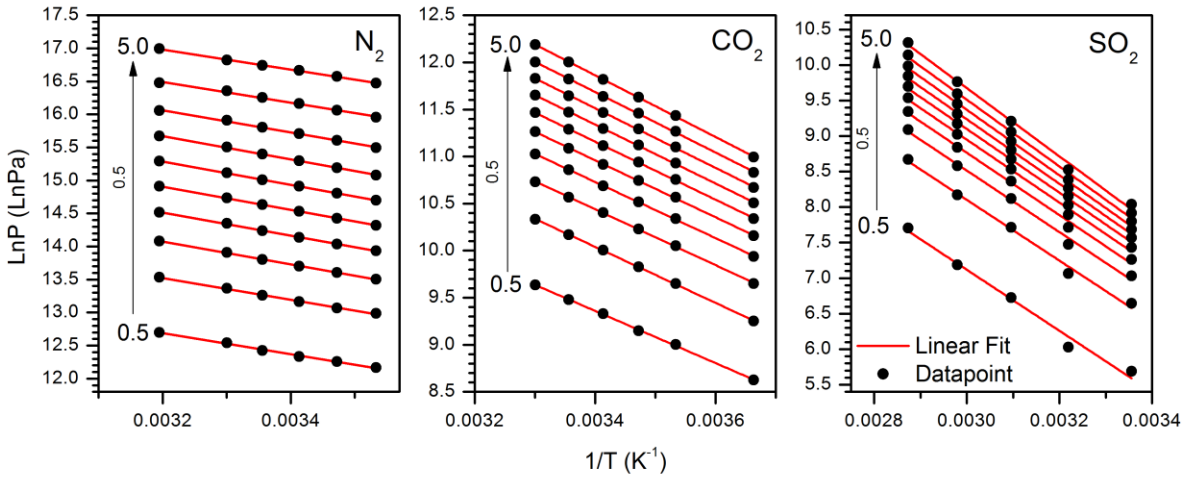

Figure S15. Linear fitting of 1/T vs LnP at intervals of 0.1 mmolg^{-1} for N_2 and 0.5 mmolg^{-1} for CO_2 and SO_2 to determine the isosteric heat of adsorption by the Van t'Hoff method.

Fitting of Isotherm Data to the Langmuir-Freundlich Model

The adsorption isotherms of N_2 and CO_2 were fitted using the single site Langmuir model;

$$n = \frac{q_{sat} b_1 P}{1 + b_1 P} \quad \textbf{(2)}$$

where n is the total amount adsorbed in mmol/g, P is the pressure in bar, q_{sat} is the saturation capacity in mmol/g and b_1 is the Langmuir parameter in bar^{-1} for the adsorption site.

The adsorption isotherms of SO_2 were fitted using the dual site Langmuir-Freundlich model;

$$n = \frac{q_{sat_1} b_1 P^{v_1}}{1 + b_1 P^{v_1}} + \frac{q_{sat_2} b_2 P^{v_2}}{1 + b_2 P^{v_2}} \quad \textbf{(3)}$$

where n is the total amount adsorbed in mmol/g, P is the pressure in bar, q_{sat_i} is the is the saturation capacity of each site in mmol/g, b_i is the Langmuir parameter for each site in bar^{-1} and v_i is the Freundlich parameter for each site.

Isotherm data collected at different temperatures were fitted simultaneously with shared q_{sat} and v_i parameters (depending on the choice of isotherm model). The regression parameters for all of the fits are above 0.99, confirming the reliability of the modelling.

Analysis and Derivation of the Ideal Adsorption Solution Theory (IAST) Selectivity

Ideal Adsorbed Solution Theory (IAST) was used to determine the selectivity factor, *S*, for binary mixtures using pure component isotherm data. *S* is defined according the equation;

$$S = \frac{x_1/y_1}{x_2/y_2} \quad \textbf{(4)}$$

where x_i is the amount of each component adsorbed, as determined by IAST and y_i is the mole fraction of each component in the gas phase at equilibrium.

The IAST adsorption selectivities were calculated for binary mixture of N_2/CO_2, N_2/SO_2 and CO_2/SO_2 of varying concentrations (50:50 to 95:5) at 298 K up to a total pressure of 1 bar. The selectivity of N_2/CO_2 and N_2/SO_2 binary mixtures are typically subject to large uncertainties due to the extremely low N_2 uptake of these materials at ambient pressures, as the IAST model must extrapolate to a pressure where the molar adsorption of both gases is comparable. The measurement of high pressure (180 bar) isotherms of N_2 in this study reduces this problem as a greater proportion of the adsorption profile is modelled, resulting in the IAST model requiring little to no extrapolation of the N_2 isotherm.

The accuracy of the IAST analysis starts to decay when;

1. strong binding sites appear on the pore surface of the material (*i.e.* the pore surface is not homogeneous).
2. in the gas mixture, one component is much more strongly adsorbed than the other.

These two criteria are broken for the adsorption of CO_2 and SO_2 compared to N_2 on MFM-300(In), and thus high pressure data have to be used.

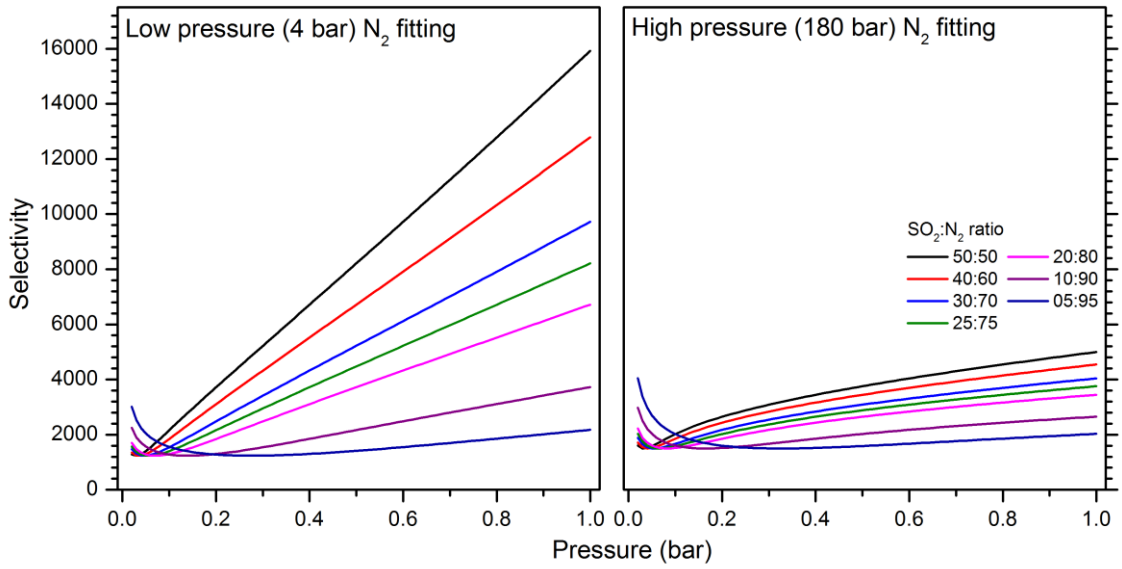

Figure S16. Comparison of effect of degree of isotherm fitting with the predicted IAST selectivity. IAST can significantly overestimate the selectivity if low pressure data for N_2 is used in the fitting. Therefore, high pressure adsorption data were used throughout this study.

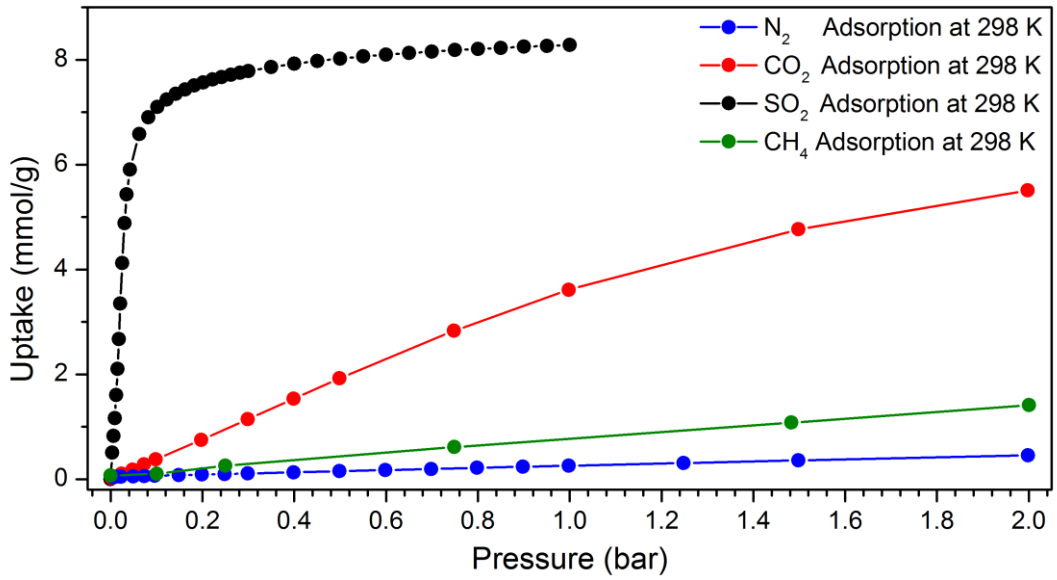

Figure S17. Comparison of N_2, CO_2, SO_2 and CH_4 adsorption isotherms of MFM-300(In) at 298 K to a pressure of 2 bar. The adsorption of methane within this material to a pressure of 2 bar was found to be significantly lower than that of CO_2 and SO_2.

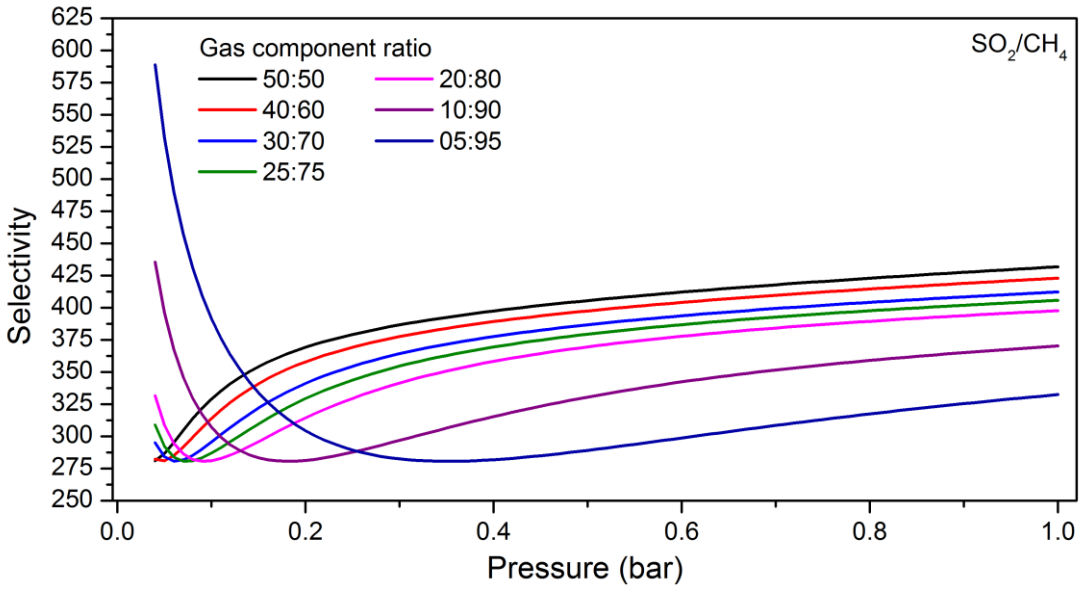

Figure S18. IAST selectivity of a range of SO_2/CH_4 mixtures to a pressure of 1 bar at 298 K.

X-Ray Powder Diffraction (PXRD) of SO_2-Loaded MFM-300(In)

Powder X-ray diffraction (PXRD) experiments on gas loaded MFM-300(In) up to a pressure of 1 bar were carried out on I11: High Resolution Powder Diffraction Beam Line at Diamond Light Source, Harwell Science Campus (UK). The diffractometer is comprised of 5 banks of 9 multi-analysing crystals (MACs) mounted 30° apart, each with coverage of 30° degrees to provide a total 2θ coverage of 0-150° using monochromatic radiation [λ = 0.826126(2) Å] from an undulator source. Temperature control was achieved by the use of an Oxford Cryosystems open-flow nitrogen gas cryostat.

A powder sample of MFM-300(In) was ground in air for 5 min before being loaded into a 0.7 mm diameter capillary tube which was glued into a brass pin. Grinding the sample provides a uniform, small particle size, essential for obtaining high quality diffraction patterns. The pin was placed into a custom goniometer head equipped with a gas inlet and mounted on the diffractometer. The sample was connected to a turbomolecular pump and outgassed at 10^{-6} mbar and 373 K for 2 h to generate the fully desolvated material, which was cooled to 298 K, dosed to 1 bar of SO_2 and X-ray data collected. The diffraction profiles were analysed initially by refining the data against the structure of bare MFM-300(In). Analysis of the Fourier difference map for bare MFM-300(In) revealed no maxima within the pore of the material, indicating complete activation of the material. The structure solution of the gas-loaded material was achieved by initially refining the data for the gas-loaded material against the structure of bare MFM-300(In). Subsequent analysis of Fourier difference maps allowed unambiguous location of the adsorbed SO_2 molecules which was added to the final refinement model. Rigid body refinement was applied to define the adsorbed SO_2 molecules in the pores. Using bond lengths and angles determined from structural data of the pure material, a global isotropic displacement parameter and occupancy were refined globally for each adsorbed gas molecule. No restraints were used to fix the position or orientation of the adsorbed SO_2 molecules.

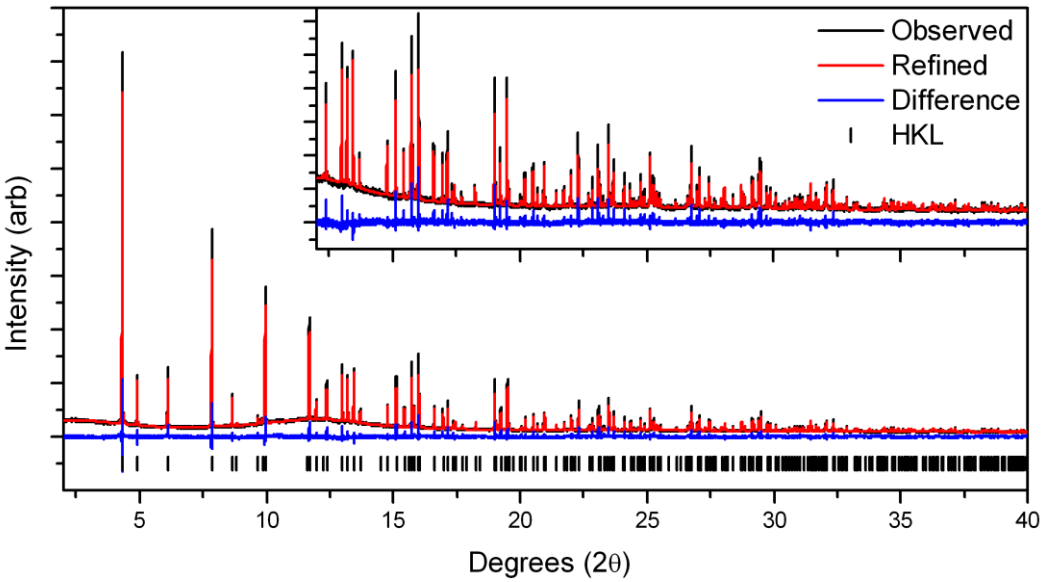

Figure S19. Observed (black), calculated (red) and difference (blue) synchrotron powder diffraction profiles for MFM-300(In) collected at λ = 0.826126 Å with a loading of 1 bar of SO_2 at 298 K; the inset shows a multiplication factor of 5x.

Crystal Structure Data

	SO_2 loaded MFM-300(In)
Chemical formula	$0.25(C_{64}H_{32}In_8O_{40})\cdot 4.0(SO_2)$
M_r	423.05
Crystal system	Tetragonal
Space group	$I4_122$
Temperature	298 K
a (Å)	15.50965 (4)
c (Å)	12.31972 (3)
V (Å^3)	2963.50 (2)
Z	8
Sample size (mm)	Cylinder, 20 × 0.7
Radiation type	Synchrotron X-Ray λ = 0.827099 Å
Scan method	Continuous scan
R_{Bragg}	3.23%
R_{wp}	6.77%
R_p	5.14%
GooF	1.57
CCDC	1475895

Table S1. Powder structural refinement parameters of SO_2 loaded MFM-300(In).

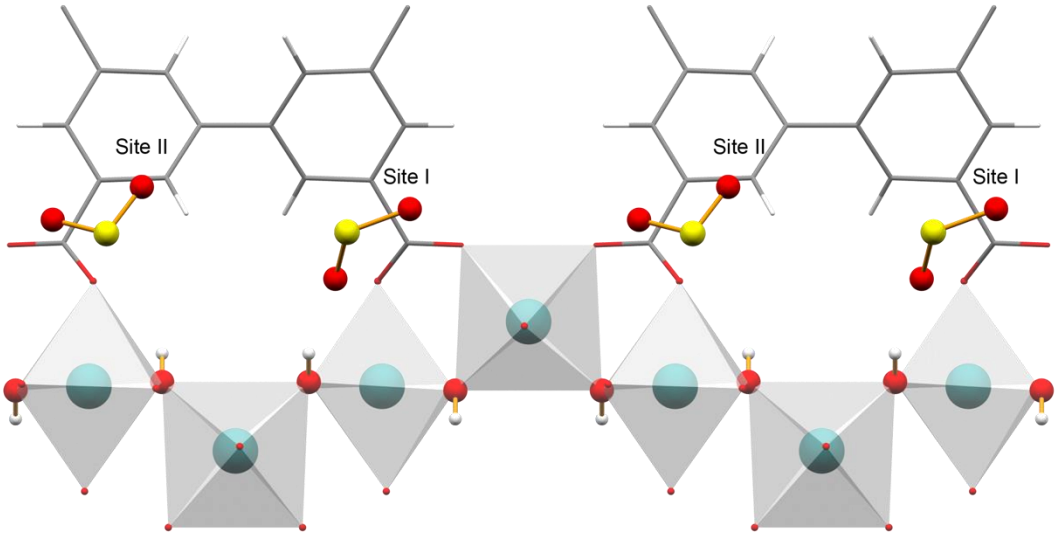

Figure S20. View of the positions of adsorbed SO_2 molecules within MFM-300(In) as determined by *in situ* powder X-ray diffraction.

X-Ray Powder Diffraction (PXRD) of High Pressure CO_2-loaded MFM-300(In)

X-Ray Powder Diffraction (PXRD) experiments of MFM-300(In) loaded with gas up to a pressure of 30 bar were carried out on ID31: High Resolution Powder Diffraction Beamline at the European Synchrotron Radiation Facility (ESRF), Grenoble (France).[3] The diffractometer is comprised of 1 bank of 9 multi-analysing crystals (MACs) mounted on a rotation stage to provide a total 2θ coverage of 0-45° using monochromatic radiation [λ = 0.495891 Å] from an undulator source. Temperature control was achieved by the use of an Oxford Cryosystems open-flow nitrogen gas cryostat.

A powder sample of MFM-300(In) was prepared as detailed above. However, in this case the sample was dosed sequentially with 10, 20 and 30 bar of CO_2. Refinement revealed no electron density within the pore of the bare material, compared with considerable electron density visible within the pore of the material upon gas loading. However, the positions of the adsorbed CO_2 molecules could not be unambiguously located, presumably due to the high pressure loading saturating the material, leading to a disordered packing arrangement.

Pawley refinement of the structure of MFM-300(In) revealed an increase in *a*/*b*, and *c* lattice parameters of 0.2 % between 0 and 30 bar, confirming the overall rigidity of the structure.

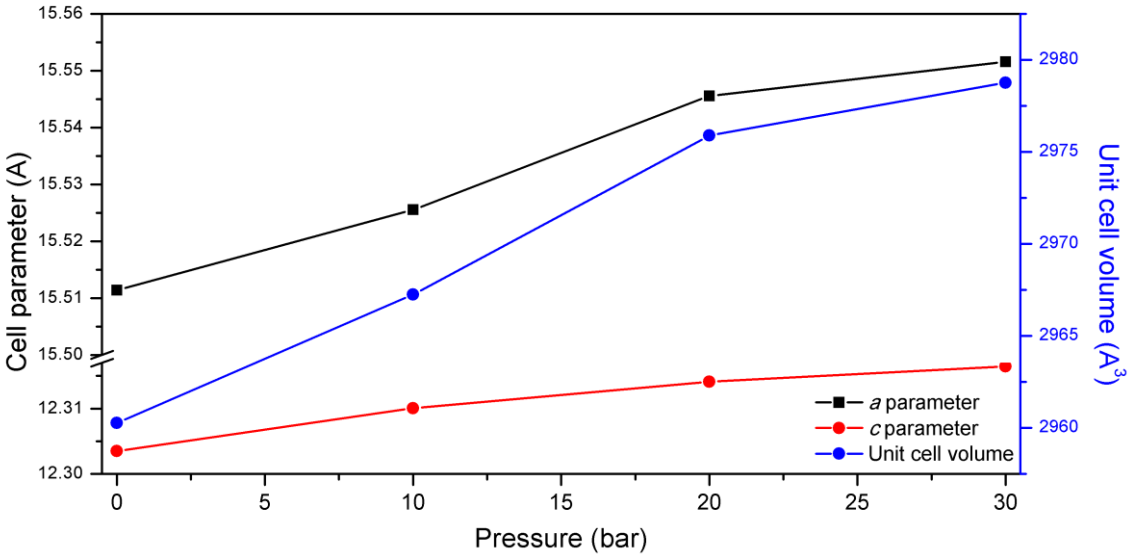

Figure S21. Changes in unit cell parameters and volume for MFM-300(In) as a function of CO_2 loading determined from the high pressure PXRD study.

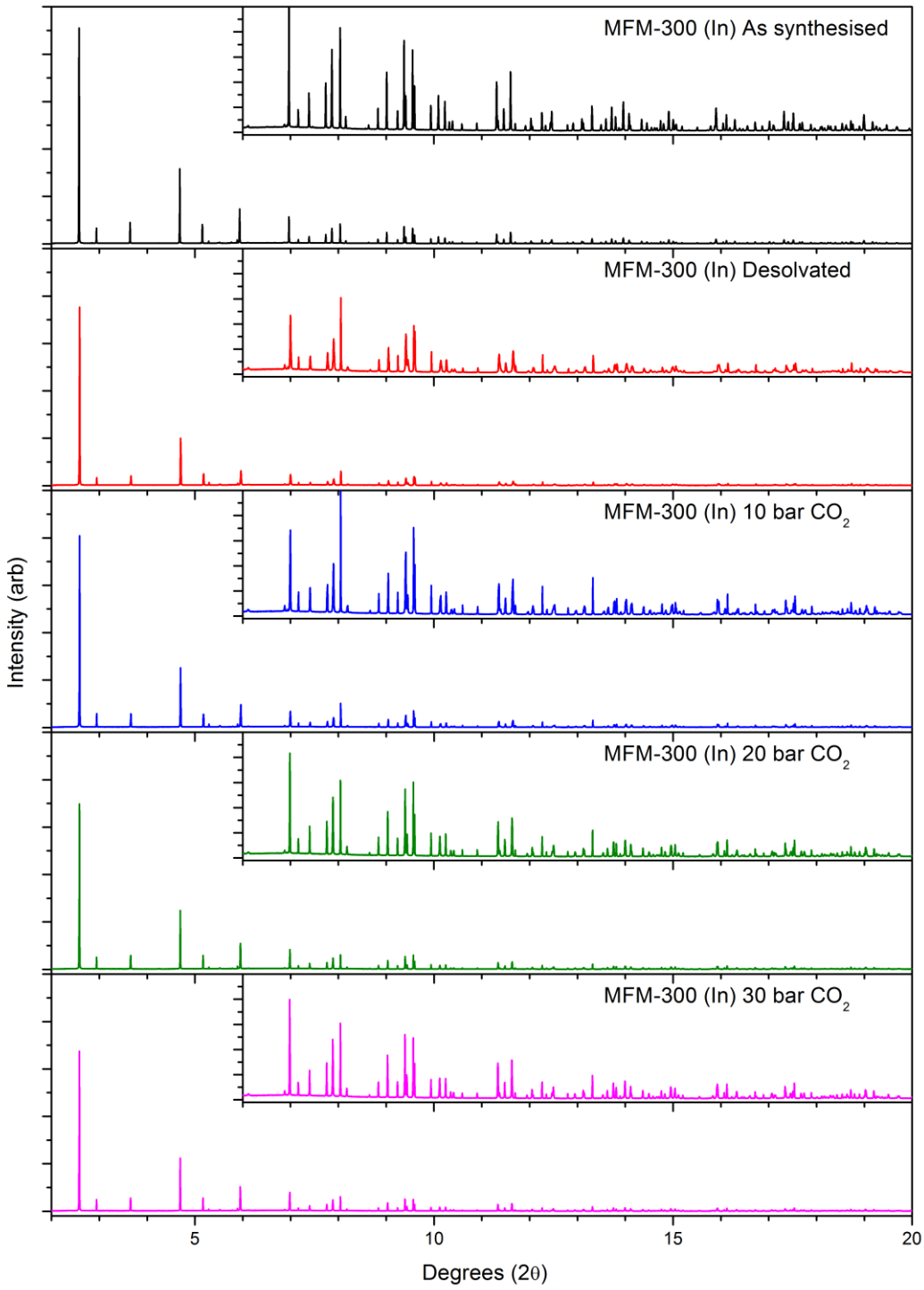

Figure S22. Comparison of PXRD patterns of MFM-300(In) collected at λ = 0.495891 Å in the as synthesised, bare and 10-30 bar CO_2 dosed states. All patterns are displayed at the same scale, with the inset figures shown at a multiplication factor of 10x.

Single Crystal X-Ray Diffraction of CO_2-Loaded MFM-300(In) at Ambient Pressure

Single crystal X-ray diffraction experiments of MFM-300(In) under vacuum and loaded with 1 bar CO_2 were carried out using the I19: Small Molecule Single Crystal Diffraction beam line at the Diamond Light Source, Harwell Science Campus, (UK). The diffractometer is comprised of a crystal-logic 4-circle diffractometer equipped with a Rigaku 742+ CCD detector using monochromatic radiation [λ = 0.6889 Å] from an undulator source. Temperature control was achieved using Oxford Cryosystems open flow nitrogen gas cryostat.

A single crystal of MFM-300(In) (200 × 100 × 100 µm) was attached to a MiTeGen MicroGripper with a minimal quantity of epoxy glue on one face of the crystal. The crystal pin was then glued into a quartz capillary gas handing cell. The cell assembly was mounted onto the goniometer and connected to a custom gas interface panel able to evacuate the cell and back fill it with as controlled pressure of a gas. Outgassing of the sample was performed using a turbomolecular pump at (base pressure 10^{-6} mbar) whilst heating the outside of the cell with a stream of N_2 gas at 423 K for 20 h. Diffraction data were collected for the crystal at 423 K. The crystal was then cooled to 298 K, dosed with CO_2 (1 bar) and cooled to 195 K while maintaining the CO_2 pressure and another dataset collected.

Structure solution was achieved by direct methods, and further developed by least squares refinements. The structure of desolvated MFM-300(In) was refined anisotropically; the hydrogen atoms were visible in the Fourier difference map and included using a riding model. In the data collection, the highest Fourier maxima was 0.7 eÅ^{-1} and located away from the bridging hydroxide group of the [$InO_4(OH)_2$] backbone of the structure; this is the location of the largest maxima in the as-synthesised material and is typically indicative of bound water. In the CO_2 loaded data collection, analysis of the Fourier difference map unambiguously reveals the location of the adsorbed CO_2 molecules, which were refined isotopically and included in the refined model. Rigid body constraints were applied to define the adsorbed CO_2 molecules, using bond lengths determined from structural data of the pure material. The occupancy and isotropic displacement parameters were refined globally for each adsorbed gas molecule and restraints were used to fix the position or orientation of the adsorbed CO_2 molecules.

Desolvated MFM-300(In)

The non-hydrogen framework atoms in the structure were refined with anisotropic displacement parameters. The framework hydrogen atoms were geometrically placed and refined using a riding model. Their isotropic displacement parameters were fixed at 1.2 x Uiso (pheny-H) or 1.5 x Uiso (O-H) of their connected heavy atoms. The largest residual electron density peak remaining in the Fourier map (height 0.64 e $Å^{-3}$) was located on a special position (0.811, 0.189, 0) 2.00 Å from atom O1. This location is inaccessible to solvent or guest molecules. No electron density peak was observed in the Fourier map for the hydroxy hydrogen atom site on O1. However, this is not unexpected for a light and mobile atom in a dataset measured at high temperature. The hydrogen atom at this position was geometrically placed and no hydrogen bond acceptor was observed in the vicinity of H1. The absolute configuration of the structure was determined by anomalous dispersion.

MFM-300(In)·4CO_2

The crystal was mounted inside a quartz environmental cell connected to a panel that can apply vacuum or load gas into the crystal. The design of the gas cell and tubing connecting it to the panel placed restrictions on the data collection strategies. These restrictions in combination with the need to omit frames of data which were badly affected by formation of ice on the outer surface of the quartz cell resulted in low completeness of 91% (to 0.95 Å) for the data. Despite the use of synchrotron radiation, truncation of the high resolution data was observed compared with the pristine crystal: a high-angle limit of 0.95Å has been applied to the data used in the refinement (SHEL). The non-hydrogen framework atoms in the structure were refined with anisotropic displacement parameters. The framework hydrogen atoms were placed geometrically and refined using a riding model. Their isotropic displacement parameters were fixed at 1.2 x Uiso (pheny-H) or 1.5 x Uiso (O-H) of their connected heavy atoms.

The CO_2 molecules were refined with isotropic displacement parameters which were refined and restrained to be similar to those of adjacent atoms (SIMU). The carbon atom of CO_2(A) lies on a special position resulting in the molecule being disordered over two symmetry-related orientations. The occupancy of the molecule was refined before being constrained such that each orientation has a

half-occupancy; the site is fully occupied. Molecule CO_2(B) lies close to a special position across which it is disordered with a mutually incompatible symmetry-related equivalent molecule. The occupancy of this molecule was refined before being constrained to have half-occupancy; the pair of symmetry related sites are occupied to the maximum allowable extent. The geometries of the two CO_2 molecules were constrained to have C-O bond lengths of 1.16 Å and O...O distances of 2.32 Å (DFIX). The largest residual electron density peak in the Fourier map has a height of 0.69 eÅ^{-3} and is located on a special position (0.75, -0.0977, 0.3750) between two sites of molecule CO_2(B). It is plausible that this electron density is associated with a third poorly defined CO_2 site related to the disorder of CO_2(B) across a different special position. Attempts were made to model this low occupancy site. However, no sensible model could be developed. The absolute configuration of the structure was determined by anomalous dispersion.

	desolvated MFM-300(In)	MFM-300(In)·4CO_2
Chemical formula	$C_{16}H_8In_2O_{10}$	$(C_{16}H_8In_2O_{10})\cdot 4(CO_2)$
M_r	587.85	765.90
Crystal Data		
Crystal system	Tetragonal	Tetragonal
Space group	$I4_122$	$I4_122$
Temperature (K)	423	195
a, *c* (Å)	15.4886 (8), 12.3439 (13)	15.352 (12), 12.226 (13)
V (Å^3)	2961.3 (4)	2882 (5)
Z (Z')	4, 0.25	4, 0.25
μ(mm^{-1})	1.59	1.55
Crystal size (mm)	0.2 × 0.1 × 0.1	0.2 × 0.1 × 0.1
Data Collection		
T_{min}, T_{max}	0.709, 1.000	0.599, 1.000
No. of measured, independent and observed [$I > 2\sigma(I)$] reflections	11453, 1701, 1642	5725, 809, 791
R_{int}	0.048	0.031
θ_{max} (°)	27.5	21.3
$(\sin \theta/\lambda)_{max}$ (Å^{-1})	0.649	0.526
$R[F^2 > 2\sigma(F^2)]$, $wR(F^2)$, S	0.025, 0.065, 1.10	0.028, 0.082, 1.21
No. of reflections	1701	809
No. of parameters	66	88
No. of restraints	0	10
	$w = 1/[\sigma^2(F_o^2) + (0.0403P)^2]$ where $P = (F_o^2 + 2F_c^2)/3$	$w = 1/[\sigma^2(F_o^2) + (0.0485P)^2 + 14.4158P]$ where $P = (F_o^2 + 2F_c^2)/3$
$\Delta>_{max}$, $\Delta>_{min}$ (eÅ^{-3})	0.64, -0.31	0.71, -0.56
Absolute structure	Flack x determined using 661 quotients [(I+)-(I-)]/[(I+)+(I-)] (Parsons, Flack and Wagner, Acta Cryst. B69 (2013) 249-259).	Flack x determined using 310 quotients [(I+)-(I-)]/[(I+)+(I-)] (Parsons, Flack and Wagner, Acta Cryst. B69 (2013) 249-259).
Absolute structure parameter	0.04 (2)	0.09 (3)
CCDC Number	1475893	1475894

Table S2. Single crystal structural refinement parameters of desolvated and CO_2-loaded MFM-300(In).

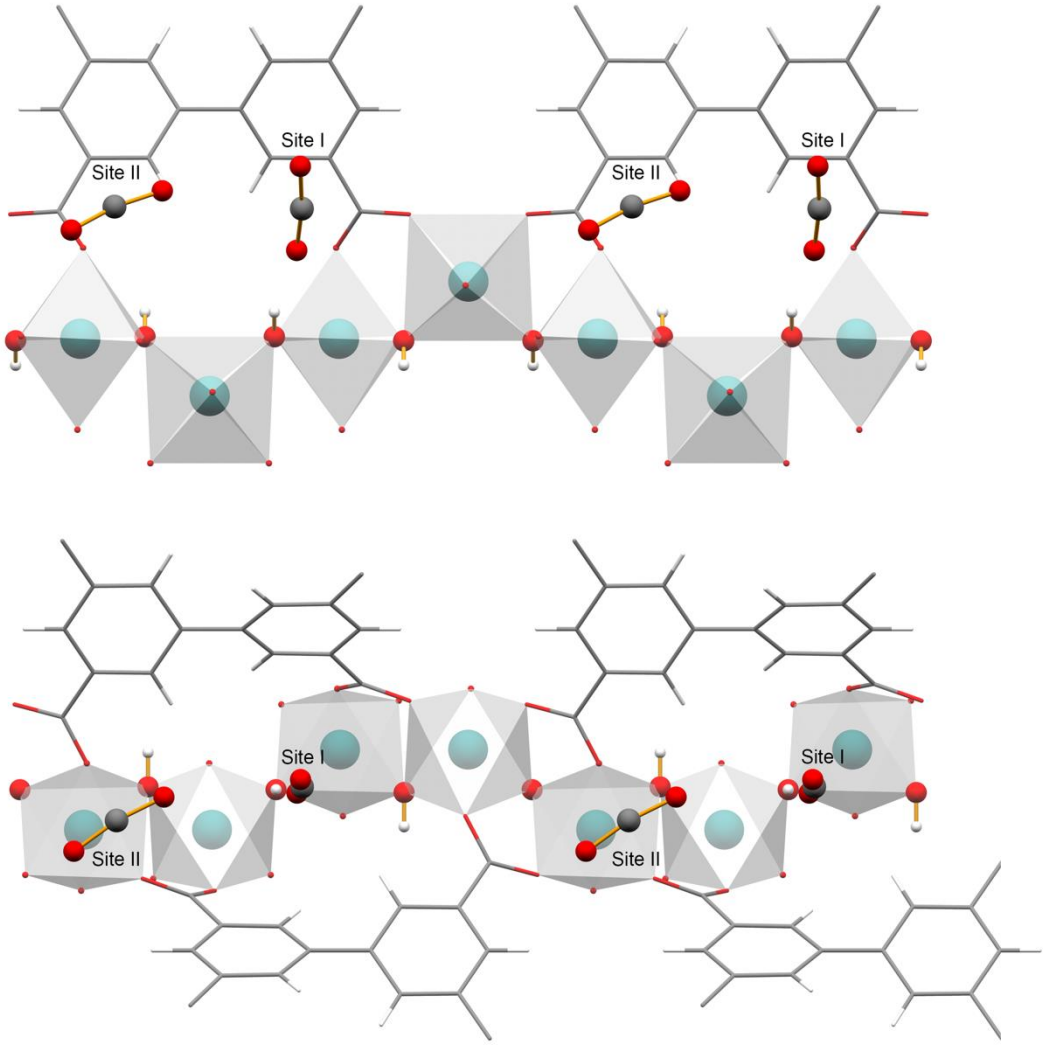

Figure S23. View of the positions of adsorbed CO_2 molecules within MFM-300(In) as determined by *in situ* single crystal X-ray diffraction.

Neutron Scattering Measurements

Inelastic neutron scattering experiments were carried out using the TOSCA spectrometer at the first target station at the ISIS Facility at the Rutherford Appleton Laboratory (UK). TOSCA is a general purpose inelastic neutron spectrometer which is able to cover the whole range of molecular vibrations from 0-400 cm^{1}. The instrument is comprised of 130 ^{3}He detectors in the forward and backscattering geometry located 17 m downstream of a 300 K Gd poisoned water moderator. A temperature of 7 ± 0.2 K was maintained during data collection by a duplex He closed cycle refrigerator with 100 mBar He as an exchange gas.

A sample of desolvated MFM-300(In) was loaded into an 11 mm cylindrical vanadium sample container, sealed with an indium vacuum seal and connected to a gas handling system. The sample was degassed at 10^{-7} mBar and 373 K for 2 days prior to the experiment to remove any remaining trace guest molecules. Gas loading was performed by a volumetric method at 298 K in order to ensure that the adsorbent was available in the gas phase and to ensure sufficient mobility within the crystalline structure of MFM-300(In). The sample was then slowly cooled to 7 K to ensure the guest molecule of interest was completely adsorbed with no condensation in the cell. Sufficient time was allowed to achieve thermal equilibrium before inelastic neutron spectra were collected to allow for full thermal equilibrium before data collection. In order to remove the adsorbed gas, the temperature of the sample cell was increased to 373 - 423 K and the gas dosed volumetrically back into dosing volume, when 95 % of the dosed gas was returned to the dosing volume, the sample was connected to a turbomolecular pump and degassed at 10^{-7} mBar and 373–437 K for 2 hours to ensure all of the guest molecules had been removed.

Modelling of INS Spectra

Density function theory (DFT) calculations were performed using CASTEP.[2] The Generalized Gradient Approximation (GGA), as implemented by Perdew-Burke-Ernzerhof (PBE), was used to describe the exchange-correlation interactions. Norm-conserving pseudopotentials were employed to account for the effects of core electrons. The experimentally determined unit cell configurations of blank and dosed MFM-300(In) were used as the initial structure for the simulations. The CO_2/SO_2 sites have partial occupancy (e.g., 0.5) in the dosed MFM-300(In). To account for this properly a supercell calculation would be desirable, but too costly in practice. Instead, a single unit cell was used and the partially occupied sites were modified to be either occupied or unoccupied, according to their local environment (there needs to be either a complete CO_2/SO_2 molecule or no molecule) and symmetry (the overall probability of being occupied needs to be proportional to the actual occupancy). The atomic coordinates were then relaxed to allow minimization of the potential energy and the interatomic forces. The energy tolerance for the electronic structure calculations was 5×10^{-10} eV, and the energy tolerance for ionic relaxation was 5×10^{-9} eV. The tolerance for the interatomic forces was 0.001 eV/Å. After convergence was reached, the force constants and the dynamical matrix were obtained using the density functional perturbation theory, from which the phonon frequencies and vibrational modes were calculated. The electronic structure calculations were performed on a 2×2×2 Monkhorst-Pack grid, and the phonon calculations were performed at the gamma-point only. The aClimax software[3] was used to convert the DFT-calculated phonon results to the simulated INS spectra.

Infrared (IR) Microscopy of CO_2- and SO_2-Loaded MFM-300(In) at Ambient Pressures

Infrared micro-spectroscopy experiments were carried out using the B22: Multimode InfraRed Imaging and Microspectroscopy (MIRIAM) beam line at the Diamond Light Source, Harwell Science Campus (UK). The instrument is comprised of a Bruker Hyperion 3000 microscope in transmission mode, with a 15x objective and liquid nitrogen cooled MCT detector, coupled to a Bruker Vertex 80 V Fourier Transform IR interferometer using radiation generated from a bending magnet source. Spectra were collected (256 scans) in the range 650-4000 cm^{-1} with 4 cm^{-1} resolution and an infrared spot size at the sample of approximately 25 × 25 µm.

Single crystals of MFM-300(In) were placed onto a ZnSe disk and placed within a Linkam FTIR 600 gas-tight sample cell equipped with ZnSe windows, a heating stage and gas inlet and outlets. The He and CO_2 were pre-dried using individual zeolite filters, and SO_2 was used as received. The analysis gases were dosed volumetrically to the sample cell using mass flow controllers, the total flow rate being maintained at 100 cm^3min^{-1} for all experiments. The gases were directly vented to an exhaust system and the total pressure in the cell was therefore 1 bar for all experiments. The sample was desolvated under a flow of dry He at 100 cm^3min^{-1} and 323 K for 2 h. The sample was then cooled to 298 K under a continuous flow of He. Dry He, CO_2 and SO_2 were dosed as a function of partial pressure, maintaining a total flow of 100 cm^3min^{-1}.

CO_2 binding

The fundamental antisymmetric stretch of CO_2 at *ca.* 2350 cm^{-1} has too great an absorbance above 0.2 bar partial pressure to be used as a probe in this study.[4] However, the higher-energy combination bands $2\nu_2 + \nu_3$ and $\nu_1 + \nu_3$, centred at 3695 and 3590 cm^{-1}, are much less intense and hence are readily studied (Figure 3 and S24). These combination bands steadily increase with increasing partial pressure of CO_2, concurrently with the ν(OH) band shifting to lower energy.[5-7] Peak fitting of the ν(OH) bands and CO_2 combination bands using Lorentzian line shapes reveals that the areas of both the CO_2 combination bands and the new ν(OH) stretch at 3652 cm^{-1} increase with pressure in an almost linear manner, matching the profile of the CO_2 adsorption isotherm at 298 K (Figure S25). The

peak area of the bare-ν(OH) stretch at 3657 cm^{-1} decreases with a similar profile, reaching around 60 % of its original value at 1 bar.

SO_2 binding

A degassed sample of MFM-300(In) was treated with increasing partial pressures of SO_2 in a He carrier flow. Fitting the IR spectral peaks corresponding to the ν(OH) stretch of the bare material (3658 cm^{-1}) and two In-OH···SO_2 interactions (SO_2^{I}, 3637 cm^{-1} and SO_2^{II}, 3617 cm^{-1}) (Figure 3 and S26) reveals an immediate saturation of the new ν(OH) band corresponding to the first In-OH···OSO^{I} interaction at an SO_2 partial pressure of 0.01 bar, consistent with the sharp isotherm profile. The intensity of ν(OH) band corresponding to the bare material reduces rapidly (in line with the increase in intensity of the ν(OH)···SO_2^{I} band) and reaches the baseline at an SO_2 partial pressure of 0.1 bar. On increasing the SO_2 partial pressure further, there is a gradual increase in the peak area of the ν(OH)···SO_2^{II} band, accompanied by a gradual decrease of the initial ν(OH)···SO_2^{I} band. The profile of the fitted bands further suggests that the initial SO_2^{I} site is saturated at very low partial pressures of SO_2, followed by additional SO_2 filling into the second (SO_2^{II}) site. This generates interactions of SO_2 molecules with molecules at the initial SO_2^{I} position, therefore decreasing the population of solely In-OH···SO_2^{I} sites.

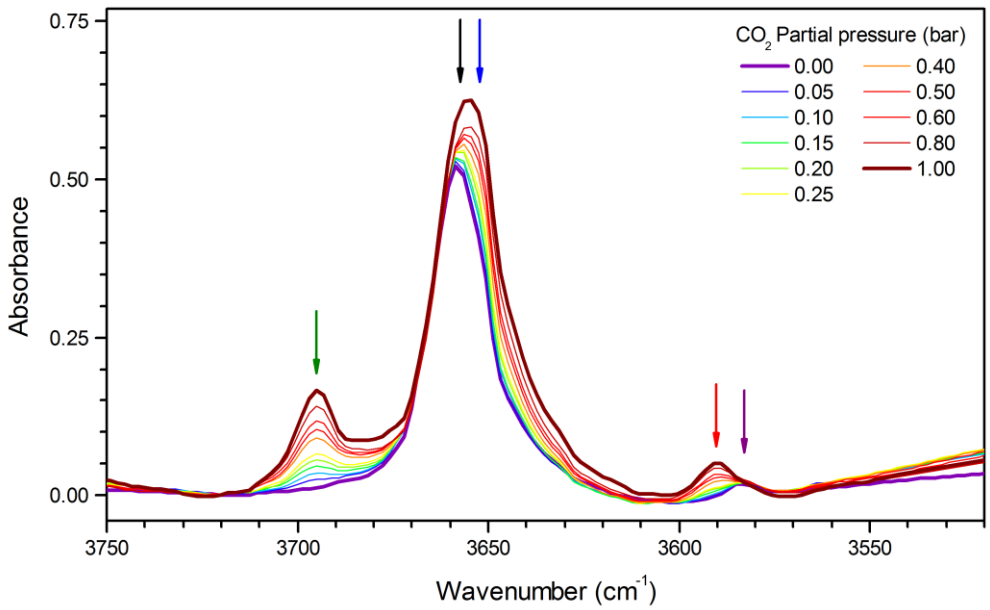

Figure S24. Stepwise CO_2 loading of MFM-300(In) at partial pressures from 0.00 - 1.00 bar in a helium carrier flow. Peak positions of the fitted Lorentzian peak shapes are shown; black, ν(OH) stretch of the bare material; blue, ν(OH) stretch of the CO_2 loaded material; green and red, CO_2 combination bands; purple, unidentified band.

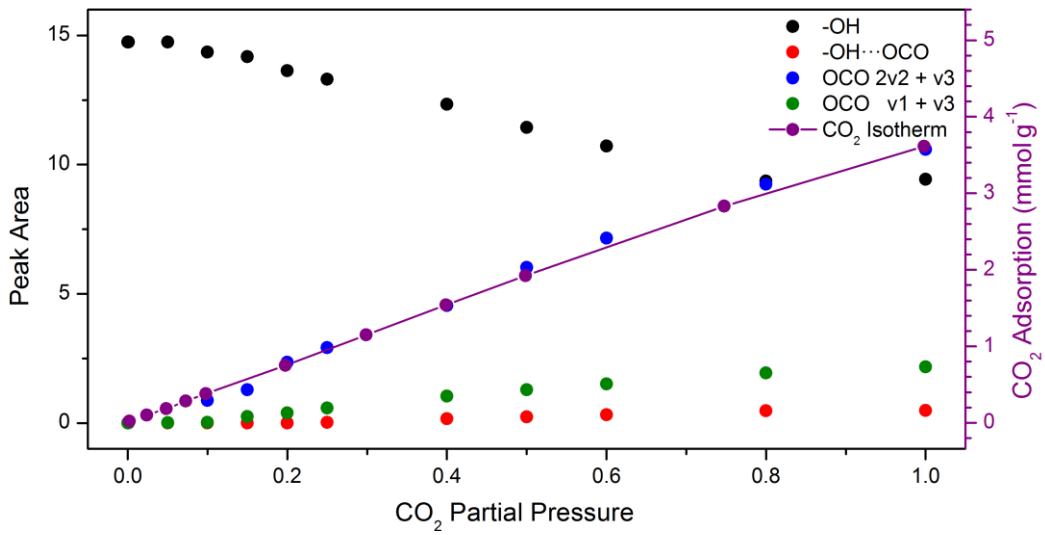

Figure S25. Fitted peak areas of the CO_2 combination bands of adsorbed CO_2 and ν(OH) of bare and CO_2-loaded MFM-300(In). A scaled CO_2 isotherm at 298 K is included for comparison with the ν(OH) stretch of the CO_2 loaded material.

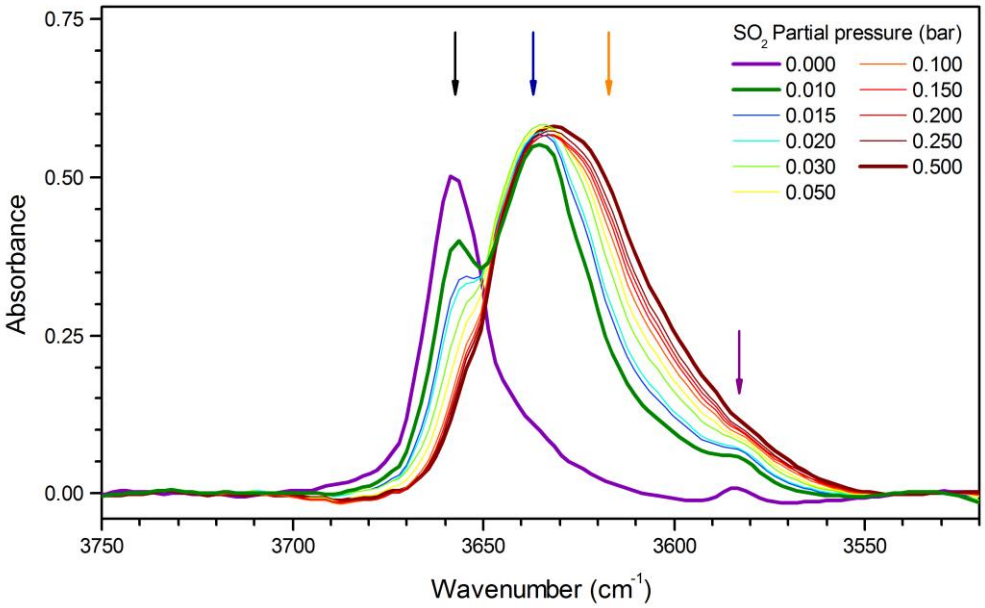

Figure S26. Stepwise SO_2 loading of MFM-300(In) at partial pressures from 0.00 – 0.50 bar. Peak positions of the fitted Lorentzian lines shapes are shown; black, ν(OH) stretch of the bare material; navy and orange, ν(OH) stretch of the SO_2 loaded material; purple, unidentified band.

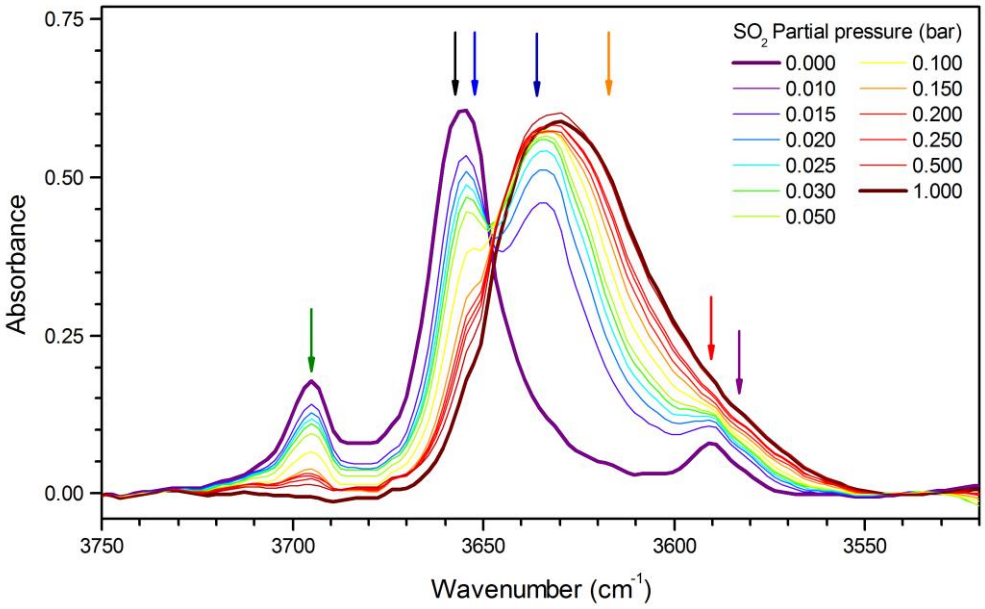

Figure S27. Stepwise SO_2 displacement of CO_2 in MFM-300(In) at partial pressures from 0.00 – 0.50 bar. Peak positions of the fitted Lorentzian lines shapes are shown; black, ν(OH) stretch of the bare material; blue, ν(OH) stretch of the CO_2 loaded material; green and red, CO_2 combination bands; navy and orange, ν(OH) stretch of the SO_2 loaded material; purple, unidentified band.

References

[1] J. Qian, F. Jiang, D. Yuan, M. Wu, S. Zhang, L. Zhang, M. Hong, *Chem. Commun*. 2012, *48*, 9696.

[2] S. J. Clark, M. D. Segall, C. J. Pickard, P. J. Hasnip, M. J. Probert, K. Refson, M. C. Payne, *Z. Kristallogr.* 2005, *220*, 567.

[3] A. J. Ramirez-Cuesta *Comput. Phys. Commun.* **2004**, 157, 226.

[4] A. Greenaway, B. Gonzalez-Santiago, P. M. Donaldson, M. D. Frogley, G. Cinque, J. Sotelo, S. Moggach, E.Shiko, S. Brandani, R. F. Howe, P. A. Wright. *Angew. Chem. Int. Ed. Eng.* **2014**, *53*, 13483.

[5] W. Yang, A. J. Davies, X. Lin, M. Suyetin, R. Matsuda, A. J. Blake, C. Wilson, W. Lewis, J. E. Parker, C. C. Tang, M. W. George, P. Hubberstey, S. Kitagawa, H. Sakamoto, E. Bichoutskaia, N. R. Champness, S. Yang, M. Schröder, *Chem. Sci*. **2012**, 3, 2993.

[6] S. Yang, L. Liu, J. Sun, K.M. Thomas, A.J. Davies, M.W. George, A.J. Blake, A.H. Hill, A.N. Fitch, C.C. Tang, M. Schröder, *J. Am. Chem. Soc.* **2013**, *135*, 4954-4957.

[7] C.P. Krap, S. Yang, R. Newby, A. Dhakshinamoorthy, H. García, I. Cebula, T.L. Easun, M. Savage, J.E. Eyley, S. Gao, A.J. Blake, W. Lewis, P.H. Beton, M.R. Warren, D.R. Allan, M.D. Frogley, C.C. Tang, M. Schröder, *Inorg. Chem.* **2016**, *55*, 1076.